International Journal of Energy and Environmental Engineering (2018) 9:383–398
https://doi.org/10.1007/s40095-018-0279-3

ORIGINAL RESEARCH

A novel time-effective model for daily distributed solar radiation estimates across variable terrain

Shaghayegh Mirmasoudi[1] · James Byrne[1] · Roland Kroebel[2] · Daniel Johnson[1] · Ryan MacDonald[1]

Received: 24 November 2017 / Accepted: 30 June 2018 / Published online: 14 July 2018

Abstract

Accurate and precisess estimation of spatio-temporal variability of solar radiation is critical. Some commonly used models evaluate this variability using methods in which the data required for estimating atmospheric attenuation may not be easily accessible for some study areas. Here, a daily solar radiation estimation method which uses ambient air temperature, a Digital Elevation Model, time of year, and monthly radiation estimates from Solar Analyst model has been proposed. The objective was to use air temperature-based empirical models for atmospheric transmissivity and diffuse fractions to vary total monthly radiation estimation from Solar Analyst, and then calculate total daily radiation as a fraction of total monthly radiation by applying a daily transmissivity-based ratio, as air temperature data are readily available at most locations on the planet. Results revealed that daily solar radiation can be estimated very well, with Mean Absolute Bias Error of around 40–53 W m^{-2} or Mean Bias Error of ± 10%, under all sky conditions at seven sites in diverse climate regions, using significantly less input data. The presented method is an improvement over previously used methods with Mean Bias Error of under 10% but more input parameters. Furthermore, the hourly solar radiation values can be calculated using the presented method using the ratio between daily and hourly radiation, for example from literature values and estimated daily insolation. The result also showed that the method is more useful for those stations with substantially higher numbers of sunny days than cloudy or partly cloudy days because the uncertainty of the model decreased from cloudy to sunny sky conditions. The implemented Digital Elevation Models environment of this method makes it applicable in many studies that need spatial estimation of solar radiation, especially for solar energy generation projects.

Keywords Solar radiation · Digital elevation model · Solar analyst · Atmospheric transmissivity · Air temperature

Abbreviations

BSRN	Baseline surface radiation network
DEM	Digital elevation model
GCOS	Global climate observing system
MABE	Mean absolute bias error
MBE	Mean bias error
SURFRAD	Surface radiation budget network
WCRP	World climate research program
WMO	World meteorological organization

✉ Shaghayegh Mirmasoudi
mirmasoudi@uleth.ca

[1] University of Lethbridge, Alberta Water and Environmental Science Building, 4401 University Drive, Lethbridge, AB T1K 3M4, Canada

[2] Lethbridge Research and Development Centre, Lethbridge, AB T1J 4B1, Canada

Variables

A	Maximum clear sky atmospheric transmissivity in Bristow and Campbell (1984) model
B	Partitioning of energy held constant at 2.4 in Bristow and Campbell (1984) model
a and b	Variables dependent on sunset hour angle in ratio of hourly to daily global radiation
C	Partitioning of energy related to monthly mean ΔT in Bristow and Campbell (1984) model
D	Number of days of year starting from first January in solar declination equation
D_R	Direct solar radiation, beam radiation, solar radiation traveling on a straight line from the sun down to the Earth's surface (Wh m^{-2})
F_R	Diffuse radiation, sky radiation, solar radiation reaching the Earth's surface after having been scattered from direct solar radiation by atmospheric particulates (Wh m^{-2})

G_R	Total amount of global solar radiation, sum of direct and diffuse radiation (Wh m^{-2})
$G_{R_{d_{TRAD}}}$	Total daily global solar radiation (Wh m^{-2}) in TRAD model
G_{R_m}	Total monthly global solar radiation used in TRAD model, calculated by Solar Analyst (Wh m^{-2})
G_{sc}	Solar constant, 1367 W m^{-2} used in extra-terrestrial radiation calculation
H_0	Extra-terrestrial solar radiation, solar radiation outside of the Earth's atmosphere (W m^{-2})
K_T	Atmospheric transmissivity, the proportion of daily solar radiation reaching the Earth's surface to the daily extra-terrestrial solar radiation
$K_{T_{d_{B-C}}}$	Daily atmospheric transmissivity used in TRAD model calculated by Bristow and Campbell (1984) model
$K_{T_{d_{B-C\,(sl)}}}$	Daily atmospheric transmissivity calculated by Bristow and Campbell (1984) model at sea level used in Solar Analyst model
K_D	Diffuse fraction, fraction of global normal radiation flux that is diffused
$K_{D_{d_{Ca}}}$	Daily diffuse fraction calculated by Carroll (1985) model
n	Total number of observations in MBE and MABE equations
r	Pearson correlation coefficient
r_G	Ratio of hourly to daily global solar radiation
t_{lapse}	Temperature lapse rate, 0.00008 m^{-1} in Solar Analyst model
x_i	i_{th} Measured value in *MBE* and *MABE* equations
y_i	i_{th} Calculated value in *MBE* and *MABE* equations
Z	Elevation above sea level (m) used in calculation of atmospheric transmissivity at sea level
ΔT	Difference between maximum and minimum air temperature (°C) in Bristow and Campbell (1984) model
$\overline{\Delta T}$	Monthly mean ΔT (°C) in Bristow and Campbell (1984) model
ϕ	Latitude of site (degrees) used in extra-terrestrial radiation calculation
ω	Hour angle, angular displacement of the sun east or west of the local meridian due to rotation of the Earth on its axis at 15 degrees per hour, morning negative, afternoon positive (degrees) used in extra-terrestrial radiation calculations
ω_s	Sunset hour angle from horizontal (degrees) used in ratio of hourly to daily global radiation and extra-terrestrial radiation calculation
$\sum_{d=1}^{n} K_{T_{d_{B-C}}}$	Sum of all days, atmospheric transmissivity values in a month calculated by Bristow and Campbell (1984) model used in TRAD model
δ	Solar declination (degrees) used in ratio of hourly to daily global radiation and extra-terrestrial radiation calculation
τ	Direct atmospheric transmissivity, proportion of extra-terrestrial radiation transmitted as direct radiation at sea level along the shortest atmospheric path

Terms

Irradiance	Instantaneous solar energy received on a unit area per unit time (W m^{-2})
Irradiation	The amount of solar energy arriving on a unit area over a stated time interval (Wh m^{-2})

Introduction

Solar radiation is a driver of photosynthesis and evapotranspiration and could become one of the most important sources of electrical energy in the near future [1, 2]. Accurate estimation of spatially continuous long-term solar radiation data is necessary information for solar electricity projects, building design processes, irrigation scheduling strategies, hydrologic models, crop simulation models, and different land management techniques such as reforestation.

Collecting radiation data in most countries is costly, difficult, and involves uncertainties, so solar radiation data are usually only recorded by a few meteorological stations [3]. For this reason, over the last few decades, many models have been developed for representing the spatio-temporal variability of global solar radiation that are applied in design and planning of solar energy systems, including recent satellite-based models, or predictive models based on correlations of solar radiation with sunshine duration, air temperature, cloud observations, and other weather data (Table 1). These spatial models are based on solar geometries and take into account site latitude, local topography, and shadowing

Table 1 A brief summary of the spatially based solar radiation models, their corresponded errors and testing locations

Model	MBE (%)	Main inputs	Testing locations
Bird [4–6]	8.0	Air mass, surface albedo, surface air pressure, precipitable water vapor, ozone	Sun-photometric sites
CEM [5, 7]	5.0	Surface albedo, surface air pressure, precipitable water vapor, cloud observations	US
ESRA [5, 6, 8]	5.0	Surface air pressure, Linke index	Europe
Ineichen [6, 9]	2.0	Atmospheric aerosol optical depth, precipitable water vapor	Europe
METSTAT [5, 6, 10]	5.0	Cloud observations, aerosol optical depth, precipitable water vapor, ozone, surface albedo, snow depth, days-since-last snowfall, atmospheric pressure	US
MRM5 [5, 6, 11, 12]	5.0	Sunshine fraction, dry- and wet-bulb temperature	UK, Japan, Europe
NSRDB—SUNY [13]	5.0	Meteorological satellite images	US
Paulescu [5, 6, 14]	− 5.0	Surface air pressure, precipitable water vapor, ozone	Sun-photometric sites
RES2 81 [6, 15]	5.0	Precipitable water vapor, ozone, surface albedo, aerosol albedo, atmospheric pressure	Sun-photometric sites
r.sun [16, 17]	− 4.5	Linke index	Spain
Solei32 [17, 18]	− 4.5	Linke index	Spain
Solar Analyst [17, 19, 20]	− 25.0	Direct atmospheric transmissivity, diffuse fraction (default values)	Spain
SRAD [17, 21]	10.0	Monthly average sunshine fraction and cloudiness data	Spain
Zelenka [22]	10.0	Meteorological satellite images	Switzerland, US

effects. However, they use different methods to calculate solar radiation, and they need different data for implementing atmospheric attenuation (Table 1).

Atmospheric attenuation often varies substantially with surface radiation. However, most locations lack long-term accurate radiation, cloudiness, and/or satellite data for many climate stations, which are needed in order to identify and estimate atmospheric attenuation. For example, models such as r.sun [16, 17], Solei-32 [17, 18] and, ESRA [5, 6, 8] calculate the overcast radiation from clear sky values and a clear-sky index called Linke (Table 1, [23, 24]). The Linke must be derived from one of the three methods: (1) from the ratio between measured global radiation and computed values of clear sky global radiation, (2) from other climatologic data such as cloudiness [23], or (3) directly from shortwave surface irradiance measured by satellites [24]. Although satellite-based models may be suitable for solar radiation estimation in large regions, their disadvantages are high cost and lack of historical records, because these methods are comparably new [25].

Sunshine duration is recognized as the most widely used meteorological parameter for solar radiation estimation, in the literature. This variable is more available and gives relatively better results than other variables [26]. However, air temperature data can be used instead, when the sunshine duration is not available at a specific location [27] as air temperature data have been collected at many locations globally and generally for a much longer period relative to any meteorological records [28].

However, using only air temperature, or air temperature along with wind speed or relative humidity data, to predict solar radiation may result in better estimation of solar radiation in clear sky conditions (higher solar radiation values) compared with cloudy sky conditions (lower solar radiation values) [29, 30]. When hourly or other short-term estimation of solar radiation is necessary, for example for solar energy production processes, it may be more practical to start with daily estimations and calculate hourly values form daily values [31]. However, the method of decomposing hourly solar radiation values from daily values also performs well for clear days [29, 30]. Nonetheless, the error caused in cloudy sky (lower solar radiation) conditions may not be very important when using the model for applications such as solar energy generation, because power generation is relatively small in these kinds of conditions and clear days produce most of the outputs from these systems [30]. In those applications, the number of sunny versus cloudy days would be a well-known variable, already taken into account.

Furthermore, empirical models, either unified and continuous or as combinations of empirical models for certain ranges, can estimate solar radiation for specific climate or specific region, because they use empirical coefficients estimated using correlations between global solar radiation and other climate variables for that specific area [27]. Accurate and simple models that are applicable for different types of climates or regions have been used in this way.

According to the spatially based solar radiation models' average uncertainty reported in Table 1, all these models are comparable with the measured values with a mean bias error (MBE) of about − 5 to 10% except Solar Analyst [17, 19, 20] that shows an under-estimation of about 25% relative to the corresponded observed values and also its reliability decreases in cloudy sky conditions. Myers (2005) [32] reviewed uncertainties in several solar radiation models and concluded that the best model uncertainties are representing the uncertainties in existing measured data which is corresponded to the mean absolute bias error (MABE) of 25–100 W m^{-2}. However, developing models with fewer input parameters under different climate conditions remains a challenge [32].Therefore, a daily global solar radiation model, within the usual range of accuracy, with lower input parameters, with more available input data, and suitable for different climate conditions applied to estimate daily and hourly solar radiation convergence curves can be usefully applied for accurate estimation of solar energy production.

Solar Analyst [17, 19, 20], which has been implemented as a tool in ESRI ArcGIS, estimates solar radiation for any geographical locations specified by a latitude and longitude or for any study area as a sum of Direct Radiation (D_{R}) and Diffuse Radiation (F_{R}) [20]. More specifically, Solar Analyst [17, 19, 20] considers atmospheric attenuation using direct atmospheric transmissivity (τ), defined as the proportion of extra-terrestrial radiation (H_0) transmitted as direct radiation at sea level along the shortest atmospheric path, and diffuse fraction (K_{D}), which is the fraction of global normal radiation flux that is diffused [20].

Here, we present a daily solar radiation estimation method which uses ambient air temperature, a Digital Elevation Model (DEM), time of year, and monthly radiation estimates from Solar Analyst ($G_{\mathrm{R_m}}$) [17, 19, 20]. Our objective was to provide improved, spatially and more widely applicable estimation using air temperature-based empirical models for atmospheric transmissivity (K_{T}) and diffuse fraction to vary total monthly radiation estimation from Solar Analyst [17, 19, 20] and then calculate total daily radiation ($G_{\mathrm{R}_{d\mathrm{TRAD}}}$) as a fraction of total monthly radiation by applying a daily transmissivity-based ratio using TRAD (temperature-estimation of radiation) daily model, as air temperature data is readily available at most locations on the planet. Our model stems from the observation that the difference between maximum and minimum air temperature (ΔT) has a strong correlation with daily average shortwave radiation [33]. Furthermore, hourly solar radiation can be decomposed from the daily values using a ratio between daily and hourly radiation [34, 35].

Methods

TRAD (temperature-estimation of radiation) daily model

Our presented TRAD daily model assumed that the daily variations in irradiation for each month are a function of daily variations in atmospheric transmissivity, the proportion of daily irradiance reaching the earth's surface to the daily extra-terrestrial insolation, in the same month. Irradiation is the amount of solar energy arriving on a unit area over a stated time interval (Wh m^{-2}) [36]. We proposed TRAD model to estimate daily irradiation values in any ground station by Eq. 1:

$$G_{\mathrm{R}_{d\mathrm{TRAD}}} = \left[K_{\mathrm{T}_{d\mathrm{B-C}}} \Big/ \sum_{d=1}^{n} K_{\mathrm{T}_{d\mathrm{B-C}}} \right] \times G_{\mathrm{R_m}} \quad (1)$$

where $G_{\mathrm{R}_{d\mathrm{TRAD}}}$ is the irradiation for the day in question (Wh m^{-2}), $K_{\mathrm{T}_{d\mathrm{B-C}}}$ is the corresponding atmospheric transmissivity of that day calculated using the Bristow and Campbell (1984) model [33] by only using maximum and minimum air temperature inputs, $\sum_{d=1}^{n} K_{\mathrm{T}_{d\mathrm{B-C}}}$ is sum of all days atmospheric transmissivity values in the corresponding month, and $G_{\mathrm{R_m}}$ is the total monthly irradiation (Wh m^{-2}) from Solar Analyst [17, 19, 20]. $G_{\mathrm{R_m}}$ is estimated using a DEM, latitude and longitude of the study location and, average annual $K_{\mathrm{T}_{d\mathrm{B-C}}}$ at sea level $\left(\left(K_{\mathrm{T}_{d\mathrm{B-C(sl)}}}\right)\right.$ [33] and also average annual daily diffuse fraction calculated by Carroll (1985) model $\left(K_{\mathrm{D}_{d\mathrm{Ca}}}\right)$ [37].

Values of $G_{\mathrm{R}_{d\mathrm{TRAD}}}$(Wh m^{-2}) were calculated for different study locations for their available observed daily irradiance (W m^{-2}) record period. Daily irradiance (W m^{-2}), instantaneous energy received on a unit area per unit time [36] was calculated from $G_{\mathrm{R}_{d\mathrm{TRAD}}}$ (Wh m^{-2}). Following, we bring descriptions of daily atmospheric transmissivity and diffuse fraction models [33, 37] and also Solar Analyst [17, 19, 20] which is used in the daily irradiation estimation using TRAD.

Daily atmospheric transmissivity and diffuse fraction models

Daily atmospheric transmissivity using the Bristow and Campbell (1984) model used to estimate daily diffuse fraction using Carroll's model [37]. $K_{\mathrm{T}_{d\mathrm{B-C}}}$ and $K_{\mathrm{D}_{d\mathrm{Ca}}}$ then used to calculate average annual $K_{\mathrm{T}_{d\mathrm{B-C(sl)}}}$ and average annual $K_{\mathrm{D}_{d\mathrm{Ca}}}$ in order to estimate $G_{\mathrm{R_m}}$ values using Solar Analyst [17, 19, 20] (Eq. 1). Then, $K_{\mathrm{T}_{d\mathrm{B-C}}}$ and $G_{\mathrm{R_m}}$ were used in TRAD model to calculate $G_{\mathrm{R}_{d\mathrm{TRAD}}}$.

Bristow and Campbell (1984) [33] proposed the following model for daily atmospheric transmissivity using the difference between maximum and minimum air temperature (ΔT):

$$K_{\mathrm{T}_{d\mathrm{B-C}}} = A \times \left(1 - \exp\left(-B \times \Delta T^{C}\right)\right) \quad (2)$$

In this equation, A, B, and C are empirical coefficients. Although empirical in nature, these coefficients represent the physics involved in the relationship, where A represents the maximum clear sky atmospheric transmissivity characteristics of the study region, which varies with elevation and pollution content of the air. Bristow and Campbell (1984) [33] developed and tested their method using data from three different sites in the northwestern United States and showed that this method provides accurate estimates of daily atmospheric transmissivity at these stations. Thornton and Running (1998) [38] reformulated the Bristow–Campbell model [33] using daily measured temperature, humidity, and precipitation to calculate daily solar radiation in 40 stations in locations with different climates. Their model gives a spatially and temporally variable estimation of A. However, Bristow and Campbell (1984) [33] used a constant value of A over all their study stations. B and C display the partitioning of energy which is characteristic of the region of interest. Bristow and Campbell (1984) [33] found it adequate to hold C constant at 2.4 for their study sites and consider B related to monthly mean ΔT via Relation 3:

$$B = 0.036 \times \exp\left(-0.154 \times \overline{\Delta T}\right) \tag{3}$$

In our study, A, B and C were applied as they were used in Bristow and Campbell (1984) [33]. $K_{T_{d_{B-C}}}$ was corrected based on elevation of the stations by the following equation, in order to use in Solar Analyst to estimate G_{R_m} [17, 19, 20]:

$$K_{T_{d_{B-C(sl)}}} = K_{T_{d_{B-C}}} - (t_{lapse} \times Z), \tag{4}$$

where $K_{T_{d_{B-C\,(sl)}}}$ is the atmospheric transmissivity at sea level, t_{lapse} is typically equal to 0.00008 m^{-1} and Z is elevation in m above the sea level [21, 39].

Liu and Jordan (1960) [34] suggested that diffuse fraction should be a well-behaved function atmospheric transmissivity. Carroll (1985) [37] proposed two relations for diffuse fraction based on atmospheric transmissivity. We used atmospheric transmissivity from Bristow and Campbell (1984) [33] model in Carroll's model [37]. The following equations show how we estimated diffuse fraction using Carroll's model [37] and $K_{T_{d_{B-C}}}$.

$$\text{for cloud} - \text{free conditions: } K_{D_{d_{Ca}}} = 0.88 - 1.024 \times K_{T_{d_{B-C}}}. \tag{5}$$

$$\text{and for cloudy conditions: } K_{D_{d_{Ca}}} = \min \begin{cases} 1.11 - 1.16 \times K_{T_{d_{B-C}}} \\ \text{or} \\ 1.0 \end{cases}. \tag{6}$$

We applied the thresholds proposed by Colli et al. (2016) [40] for classification of daily average sky conditions of a ground station (Table 2). The model was evaluated for three different groups of days based on different sky conditions including cloudy days, partly cloudy days and sunny or clear days (Table 2).

Application of solar analyst

Total annual global solar radiation in monthly intervals $\left(G_{R_m}\right)$ was calculated using Solar Analyst [17, 19, 20] by a DEM, latitude and longitude of the study location and also, average annual $K_{T_{d_{B-C(sl)}}}$ and average annual $K_{D_{d_{Ca}}}$.

Four calculations are contained in the upward-looking hemispherical algorithm applied in Solar Analyst [17, 19, 20]: viewshed, sunmap, skymap calculation, and a concluding calculation that uses the previous three calculations to estimate a solar radiation value. The total amount of global solar radiation in Wh m^{-2} is obtained by the sum of direct solar radiation (Wh m^{-2}) for all sunmap sectors and diffuse solar radiation for all skymap sectors (Wh m^{-2}) [20]. The direct solar radiation from a sunmap sector with a centroid at solar zenith angle (degrees) and solar azimuth angle (degrees) is a function of the solar constant (1367 W m^{-2}), τ, the elevation above sea level (meters), the time duration represented by the sky factor, the surface zenith angle (degrees), the surface azimuth angle (degrees), and the gap fraction for the sunmap sector. Correspondingly, diffuse solar radiation for each sky sector at the same centroid is related diffuse fraction, the elevation above sea level (meters), the bounding zenith angles of the sky sector (degrees), the number of azimuthal divisions in the sky map, the time interval for analysis, fraction of visible sky for the sky sector, and the angle of incidence between the centroid of the sky sector and the intercepting surface (degrees). However, providing a correct value for τ is difficult because it is sensitive to the presence of clouds [17]. For this reason, we applied $K_{T_{d_{B-C(sl)}}}$ and $K_{D_{d_{Ca}}}$ in the calculation of G_{R_m} using Solar Analyst [17, 19, 20].

Table 2 Daily atmospheric transmissivity thresholds for day classification [40]

Daily atmospheric transmissivity	Day classification
Daily atmospheric transmissivity ≤ 0.30	cloudy
0.30 < daily atmospheric transmissivity < 0.50	partly cloudy
Daily atmospheric transmissivity ≥ 0.50	sunny and clear

Observed daily atmospheric transmissivity

In the present study, observed daily atmospheric transmissivity on a horizontal surface was calculated using Eq. 7 which defines atmospheric transmissivity $\left(K_{\mathrm{t}}\right)$ as a ratio of a day's radiation $\left(G_{\mathrm{R}}\right)$ to that day's extra-terrestrial radiation (H_0)

$$K_{\mathrm{t}} = \frac{G_{\mathrm{R}}}{H_0}. \tag{7}$$

The value of G_{R} (W m^{-2}) is provided using the available pyranometer measurements, but H_0 (J m^{-2}) is calculated by the following method [41]

$$H_0 = \frac{24 \times 3600 G_{\mathrm{sc}}}{\pi}\left(1 + 0.033\cos\frac{360n}{365}\right) \times \left(\cos\phi\cos\delta\sin\omega_{\mathrm{s}} + \frac{\pi\omega_{\mathrm{s}}}{180}\sin\phi\sin\delta\right) \tag{8}$$

G_{sc} is the solar constant (1367 W m^{-2}), D is the number of the day of the year starting from January 1 = 1, and ϕ is the latitude. H_0 then converted to W m^{-2} to use in Eq. 7.

The declination δ is found from the equation below [41] (23.45 is the Earth's rotational axis vector to the ecliptic plane in degrees):

$$\delta = 23.45\sin\left(360\frac{284 + D}{365}\right). \tag{9}$$

The sunset hour angle ω_{s} in degrees from horizontal is calculated using the following equation [41]:

$$\cos\omega_{\mathrm{s}} = -\tan\phi\tan\delta. \tag{10}$$

Hourly solar radiation model

Accurate hourly solar radiation data are necessary in many studies, for example in solar photovoltaic projects. We can apply a ratio to the estimated daily solar radiation values from the previous steps (Eq. 11) and decompose the hourly solar radiation values. Liu and Jordan (1960) [34] improved the study by Whillier (1956) [42] to calculate the ratio of hourly to daily global solar radiation using a set of regression curves. Collares-Pereira and Rabl (1979) [31] validated their approach and presented Eq. 11 for estimating this ratio, which only needs site latitude and day number;

$$r_{\mathrm{G}} = \frac{\pi}{24}(a + b\cos\omega)\frac{\cos\omega - \cos\omega_{\mathrm{s}}}{\sin\omega - \omega_{\mathrm{s}}\cos\omega_{\mathrm{s}}} \tag{11}$$

where r_{G} is the ratio of hourly to daily global radiation, a and b are dependent on sites (Eq. 12 and 13), ω is hour angle in degrees and defined as the angular displacement of the sun east or west of the local meridian due to rotation of the earth on its axis at 15°/h, morning negative, afternoon positive, and ω_{s} is the sunset hour angle in degrees that is calculated by Eq. 10.

$$a = 0.4090 + 0.5016\sin\left(\omega_{\mathrm{s}} - 1.047\right) \tag{12}$$

$$b = 0.6609 - 0.4767\sin\left(\omega_{\mathrm{s}} - 1.047\right). \tag{13}$$

Equation 11 has been developed based on data from measurement sites in the US, but it also has been validated for 13 Indian locations by Hawas and Muneer (1984) [43] and 16 sites in the UK [35].

Data availability for verification

The Surface Radiation Budget Network (SURFRAD) was established in 1993 in the US [44] and became an official part of the Global Climate Observing System (GCOS) in April 2004 [45]. Currently, seven SURFRAD stations are operating in diverse climate regions in the USA, in Montana, Colorado, Illinois, Mississippi, Pennsylvania, Nevada, and South Dakota (Table 3 and Fig. 1). The stations are not surrounded by trees or any other obstacles, but may be located in areas with small shrubs or agriculture.

An upward-looking pyranometer measures total global solar radiation (W m^{-2}) on its main platform. Accuracy of the pyranometer is about 5%, which is achieved by the standards of calibrations and operations recommended by the Baseline Surface Radiation Network (BSRN), sponsored by the World Climate Research Program (WCRP) of the World Meteorological Organization (WMO). SURFRAD data are available into daily files of one- or three-minute data. We extracted daily maximum and minimum air temperature (°C) and mean irradiance (W m^{-2}) from the one- or

Table 3 SURFRAD network information

Site Name	Latitude	Longitude	Elevation (m)	Time Zone	Installed
Bondville, IL	40.0519°N	88.3731°W	230	UTC-6	April 1994
Boulder, CO	40.1249°N	105.2368°W	1689	UTC-7	July 1995
Desert Rock, NV	36.6237°N	116.0195°W	1007	UTC-8	March 1998
Fort Peck, MT	48.3078°N	105.1017°W	634	UTC-7	November 1994
Goodwin Creek, MS	34.2547°N	89.8729°W	98	UTC-6	December 1994
Penn State, PA	40.7201°N	77.9309°W	376	UTC-5	June 1998
Sioux Falls, SD	43.7340°N	96.6233°W	473	UTC-6	June 2003

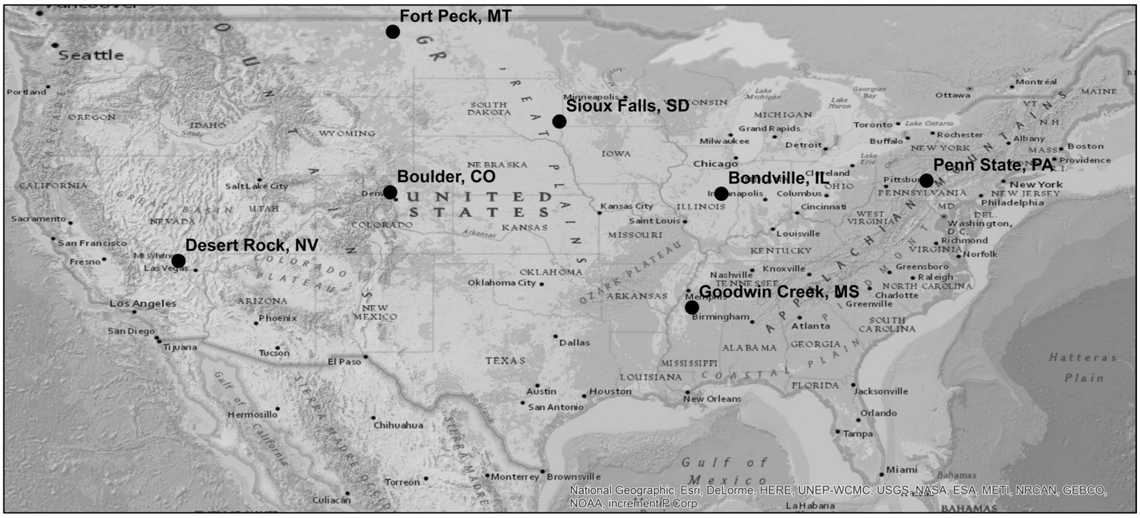

Fig. 1 A geographical map of SURFRAD stations located in the US

three-minute data records for the available historical time period at each station.

A small number of spurious values in air temperature and irradiance records were removed from the analysis. Irradiance data that had negative values due to cooling of the thermopile near dusk and dawn [45] and values higher than the extra-terrestrial solar radiation were filtered out as well. Missing data were not used in the analysis (Table 4). However, the amount of missing data was small (Table 4) as the data have already been quality controlled by SURFRAD (Table 4) [44]. Furthermore, in order to analyze the results in both a large and a small sample size in terms of years, we used 2015 as a case study. A 30 × 30 m DEM covering all the SURFRAD sites was applied [46].

The extracted observed daily maximum and minimum air temperature (°C) data were used in the proposed solar radiation method to estimate daily mean irradiance (W m^{-2}, Eqs. 1–6) in order to compare it with the observed mean irradiance (W m^{-2}) at different SURFRAD stations. The observed daily mean irradiance (W m^{-2}) was also used to find observed daily atmospheric transmissivity (Eqs. 7–10) to compare it with the calculated daily atmospheric transmissivity values from the Bristow and Campbell (1984) model [33] (Eqs. 2–4).

Statistical validation methods

In the present study, the predictive efficiency of the model was tested using the mean bias error (MBE) and the mean absolute bias error (MABE). These terms are defined by the following equations;

$$\mathrm{MBE} = \frac{1}{n}\sum_{i=1}^{n}\left(y_i - x_i\right) \tag{14}$$

$$\mathrm{MABE} = \frac{1}{n}\sum_{i=1}^{n}\left|y_i - x_i\right| \tag{15}$$

where x_i is the i th measured value, y_i is the i th calculated value, and n is the total number of observations. The MBE is a measure of the systematic error of a model. It evaluates the tendency of a model to under- or over-estimate the measured values and for an accurate model is equal to zero [47]. The MABE is a measure of the goodness of the fit for a model, and a natural measure of average error and a good test for inter-comparisons of the average model performance error. For precise data modeling, MABE should be close to zero

Table 4 The time period and data used in the study

Site Name	Time period	Total years	Missing data (%)
Bondville, IL	Jan 1996 to Dec 1998 and Jan 2000 to Dec 2015	19	0.32
Boulder, CO	Jan 1996 to Dec 2015	20	0.05
Desert Rock, NV	Jan 1999 to Dec 2011 and Jan 2013 to Dec 2015	16	0.82
Fort Peck, MT	Jan 1997 to Dec 2015	19	0.61
Goodwin Creek, MS	Jan 1996 to Dec 2002 and Jan 2005 to Dec 2015	18	0.71
Penn State, PA	Jan 1999 to Dec 2015	17	1.50
Sioux Falls, SD	Jan 2004 to Dec 2006 and Jan 2008 to Dec 2015	11	0.10

[47]. We also provide the Pearson correlation coefficient between the observed and modeled data. The Pearson correlation produces a sample correlation coefficient, r, which measures the strength and direction of linear relationships, negative or positive, between paired continuous variables.

Results and discussion

All years

Daily radiation verification

Pearson correlation test results showed a strong positive correlation between the measured and estimated irradiance values and this correlation increased from cloudy to sunny days (Table 5). However, exceptions were Fort Peck and Penn State, which had very small differences in correlation between partly cloudy and sunny days (Table 5). Considering all the stations together for the entire study years, in case of cloudy days, there was a significant positive correlation ($r=0.55$; Table 5) and partly cloudy and sunny days showed a stronger positive correlation ($r=0.85$ and $r=0.89$, respectively; Table 5).

The result showed the MABE decreased significantly from cloudy (about 112%) and partly cloudy (about 38%) to sunny days (about 18%) (Table 5). This error was more than three times larger under cloudy sky conditions than partly cloudy and more than six times larger in cloudy days than sunny days (Fig. 3b).

MBE calculations showed the model over-estimated the measured daily irradiance for cloudy days (about 88%) (Table 5; Fig. 3d). In partly cloudy conditions, the over-estimation (about 16%) slightly decreased compared to the cloudy days (Tables 5; Fig. 3d). However, clear or sunny days showed under-estimations relative to the observed values (about 8%) (Tables 5; Fig. 3d). The only exception was Fort Peck station with under-estimations on partly cloudy days (Fig. 3d).

The results showed that the model is less able to account for partly cloudy and cloudy days. However, it gives a reasonable estimation for solar radiation during the clear and sunny days, taking into account the average 8% percent under-estimation or 18% error in overall model performance. One of the likely sources of error is using a value for maximum atmospheric transmissivity of 0.7 in Bristow–Campbell model (1984) [33], although this value is known to differ with elevation and air particle content [33]. Variable maximum atmospheric transmissivity can be applied using the reformulated Bristow–Campbell model [33] by Thornton and Running (1998) [38]; however, their model uses precipitation and humidity data plus air temperature data. The MABE and MBE in estimating daily solar radiation in clear and sunny days using the presented model in this study, which are around 18 and 8%, respectively, are reasonable compared to the same errors in estimation daily solar radiation by Thornton and Running (1998) [38] which are 15 and 4%, respectively. The average MBE of our model (8%) on clear and sunny days is also within the range of MBE of the Solei-32 [17, 18], Solar Analyst [17, 19, 20], SRAD [17, 21] and r.sun [16, 17] models in the same sky condition, which is under 10%. However, our model depends mainly on air temperature data, whereas other models need accurate radiation, cloudiness, and/or satellite data as input. TRAD model (Eq. 1) is also a function of total monthly radiation estimated by Solar Analyst [17, 19, 20]. Atmospheric attenuation for calculating total monthly radiation in Solar Analyst [17, 19, 20] was applied using the estimated average annual $K_{T_{d_{B-C(sl)}}}$ and $K_{D_{d_{Ca}}}$ may affect the results and consequently the daily solar radiation estimation in TRAD model (Eq. 1). Furthermore, the accuracy of the measured data should be considered (accuracy of the pyranometer is about 5%).

Desert Rock station showed the best overall model performance (MABE about 17%) between all other stations when considering all sky conditions (Table 5). This is because this station had the highest average percentage of clear and sunny days (89%) (Fig. 2).

Daily atmospheric transmissivity verification

The Pearson correlation test between the estimated and measured daily atmospheric transmissivity values in cloudy and partly cloudy conditions applied for all the study years showed that there was a low positive correlation between the estimated and measured values in all stations, except for Desert Rock and Boulder in cloudy days and Sioux Falls in partly cloudy days (Table 5). These correlations also increased from cloudy and partly cloudy to sunny days in all stations except in Fort Peck (Table 5).

The MABE for daily atmospheric transmissivity is considerably higher for cloudy days (about 135%) than partly cloudy days (about 40%) (Table 5; Fig. 3a). The MBE test showed that the Bristow–Campbell model [33] over-estimated the measured daily atmospheric transmissivity for cloudy days (118%) (Fig. 3c). Over-estimations for partly cloudy days (about 25%) decreased compared to the cloudy days (Fig. 3c). However, clear or sunny days showed under-estimations (about 9%) (Fig. 3c). The only exception was Fort Peck station with over-estimations on partly cloudy days (Fig. 3c).

The result showed that the Bristow and Campbell (1984) [33] model gives better estimation (about 15% error) of daily atmospheric transmissivity for sunny days

Table 5 Statistical comparison of the observed daily atmospheric transmissivity and daily irradiance against the corresponding modeled values using MBE, MABE, and Pearson correlation coefficients (r) between the observed and modeled values for each study site individually, and also for all the seven sites together in their total study years (MBE and MABE in % are related to the mean observed value)

Station Name	Daily atmospheric transmissivity					Daily irradiance					n
	MBE		MABE		r	MBE		MABE		r	
	(%)		(%)			(%)	(W m^{-2})	(%)	(W m^{-2})		
All sky conditions											
Bondville, IL	6.10	0.03	26.80	0.13	0.57**	0.40	0.74	27.50	45.96	0.82**	6918
Boulder, CO	− 3.20	− 0.02	23.00	0.13	0.35**	3.30	6.35	27.70	52.63	0.78**	7301
Desert Rock, NV	− 12.50	− 0.08	19.00	0.13	0.45**	− 10.30	− 24.25	17.30	40.65	0.88**	5796
Fort Peck, MT	20.0	0.09	33.00	0.15	0.46**	-2.50	-3.90	24.80	39.87	0.88**	6897
Goodwin Creek, MS	5.80	0.03	23.00	0.11	0.62**	3.10	5.60	24.40	44.59	0.80**	6528
Penn State, PA	10.10	0.05	29.70	0.14	0.61**	9.60	14.86	30.30	47.02	0.84**	6116
Sioux Falls, SD	8.60	0.04	32.20	0.16	0.13**	1.50	2.50	27.00	44.87	0.83**	4013
Combined data from all stations	3.77	0.02	25.10	0.13	0.50**	0.28	0.49	25.27	45.26	0.83**	43569
Daily atmospheric transmissivity ≤ 0.30 (Cloudy sky)											
Bondville, IL	108.0	0.19	130.2	0.23	0.12**	89.1	44.73	111.10	55.77	0.62**	1503
Boulder, CO	135.05	0.26	148.73	0.28	NSS	145.77	89.29	157.89	96.70	0.45**	599
Desert Rock, NV	127.05	0.23	138.81	0.26	NSS	143.53	74.73	155.15	80.78	0.41**	209
Fort Peck, MT	108.11	0.22	124.99	0.25	0.22**	41.75	21.74	77.98	40.61	0.67**	1335
Goodwin Creek, MS	119.97	0.19	136.73	0.22	0.06*	106.02	52.04	124.72	61.22	0.36**	1309
Penn State, PA	90.24	0.16	115.44	0.20	0.14**	76.50	38.88	102.46	52.07	0.55**	1589
Sioux Falls, SD	198.17	0.36	201.09	0.37	0.10**	90.78	51.20	115.01	64.87	0.63**	665
Combined data from all stations	117.65	0.21	135.58	0.24	0.15**	87.79	45.68	111.65	58.09	0.55**	7209
0.30 < daily atmospheric transmissivity < 0.50 (Partly cloudy sky)											
Bondville, IL	22.16	0.08	38.44	0.15	0.18**	18.33	24.40	36.51	48.62	0.84**	1409
Boulder, CO	24.1	0.10	36.47	0.15	0.12**	33.76	46.98	44.79	62.34	0.85**	1363
Desert Rock, NV	20.88	0.08	35.18	0.15	0.15**	23.30	29.86	36.82	47.18	0.83**	429
Fort Peck, MT	34.50	0.14	48.49	0.19	0.17**	− 5.76	− 6.32	38.78	42.55	0.87**	2313
Goodwin Creek, MS	20.68	0.08	33.51	0.14	0.20**	19.84	29.41	33.40	49.51	0.78**	1180
Penn State, PA	17.04	0.06	38.26	0.15	0.22**	17.84	22.92	38.48	49.45	0.82**	1598
Sioux Falls, SD	33.98	0.13	45.93	0.18	NSS	18.20	22.36	40.60	49.90	0.85**	805
Combined data from all stations	25.48	0.10	40.49	0.16	0.16**	15.96	20.43	38.60	49.44	0.85**	9097
Daily atmospheric transmissivity ≥ 0.50 (Sunny and clear sky)											
Bondville, IL	− 7.49	− 0.04	13.90	0.09	0.22**	− 10.86	− 24.25	18.57	41.47	0.90**	4006
Boulder, CO	− 12.05	− 0.08	16.92	0.11	0.15**	− 6.15	− 13.35	20.84	45.24	0.90**	5339
Desert Rock, NV	− 15.53	− 0.11	16.99	0.12	0.27**	− 12.81	− 32.22	15.40	38.72	0.92**	5158
Fort Peck, MT	1.16	0.01	13.28	0.08	0.23**	− 5.34	− 12.91	15.60	37.72	0.87**	3249
Goodwin Creek, MS	− 6.16	− 0.04	11.82	0.08	0.30**	− 6.84	− 16.12	16.05	37.81	0.88**	4039
Penn State, PA	− 4.31	− 0.03	13.90	0.09	0.28**	− 1.16	− 2.61	19.03	42.78	0.89**	2929
Sioux Falls, SD	− 10.64	− 0.06	16.70	0.10	0.10**	− 7.90	− 16.50	18.11	37.83	0.92**	2543
Combined data from all stations	− 8.86	− 0.05	15.02	0.10	0.19**	− 7.87	− 18.13	17.63	40.61	0.89**	27263

NSS not statistically significant

*Significant at the 95% confidence level

**Significant at the 99% confidence level

than for partly cloudy or cloudy sky conditions, which also describes the performance of the daily solar radiation model using TRAD model (Eq. 1) in sunny and clear days. The average MBE of Bristow and Campbell (1984) [33] considering all study years and sky conditions together is around 4% (Table 5).

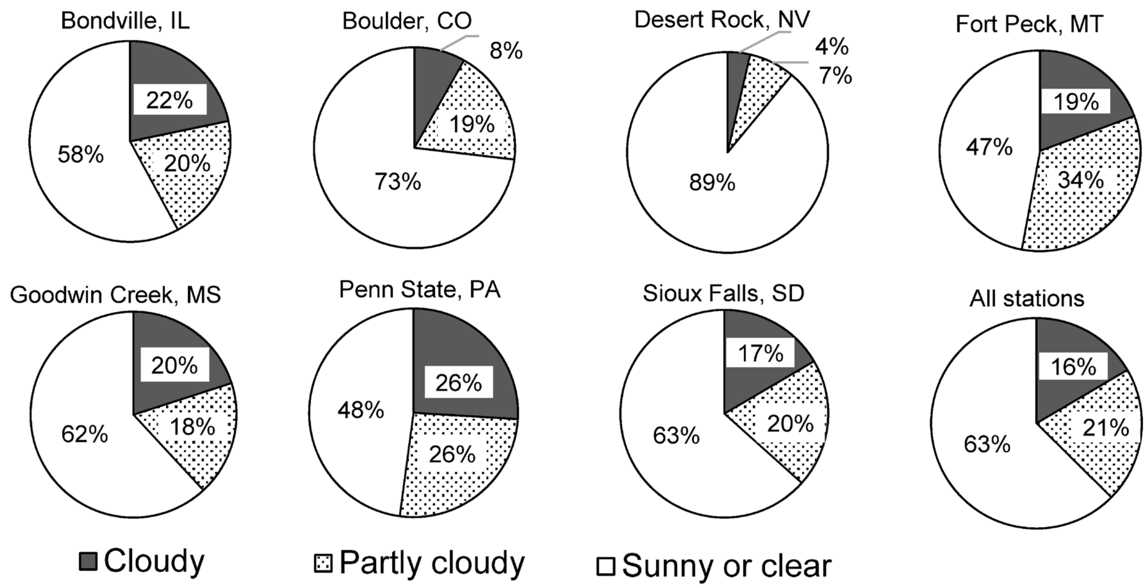

Fig. 2 Average percentage of each sky condition in different sites

Year 2015

Daily radiation verification

The result of Pearson correlation tests showed that there always was a strong positive correlation between the measured and estimated irradiance values, and this correlation increased from cloudy to sunny days in year 2015 (Table 6). However, exceptions were very small differences in correlation between partly cloudy and sunny days in Fort Peck and Penn State (Table 6).

The result showed that the MABE declined significantly from cloudy (105%) and partly cloudy (about 38%) to sunny days (17%) (Table 6). This error was more than three times higher under cloudy days than partly cloudy and more than six times higher in cloudy sky conditions than sunny (Fig. 4b).

MBE result indicated that the model over-estimated the measured daily irradiance for cloudy days (about 83%) (Tables 6; Figs. 4d and 5a–h). In partly cloudy days, the over-estimation (about 19%) decreased relative to the cloudy conditions (Table 6; Figs. 4d and 5a–h). However, clear or sunny sky condition showed under-estimations relative to the observed values (6%) (Table 6; Figs. 4d and 5a–h). The only exception was Fort Peck station with under-estimations in partly cloudy days (Figs. 4d and 5a–h).

Daily atmospheric transmissivity verification

In 2015, there was no correlation between the estimated and measured daily atmospheric transmissivity values in cloudy and partly cloudy days in any stations, except there were significant correlations in Fort Peck and Penn State in cloudy days and Goodwin Creek and Penn State in partly cloudy days (Table 6). On sunny days, there was a positive correlation in all stations except Fort Peck and Bondville (Table 6).

The MABE for daily atmospheric transmissivity was considerably higher for cloudy days (145%) than partly cloudy days (42%) (Table 6; Fig. 4a). The MBE test showed Bristow–Campbell model [33] over-estimated the measured daily atmospheric transmissivity for cloudy days (about 130%) (Fig. 4c). Over-estimations for partly cloudy days (about 28%) decreased compared to the cloudy days (Fig. 4c). However, clear or sunny days showed under-estimations (about 9%) (Fig. 4c). The only exception was Fort Peck station with over-estimations on sunny sky conditions (Fig. 4c).

Conclusions

In this study, we presented a method for estimating daily solar radiation using only maximum and minimum air temperature, topography, and time of year. We designed the method based on TRAD, a daily solar radiation model that used estimated daily atmospheric transmissivity from the Bristow and Campbell (1984) [33] model and calculated total monthly solar radiation values by Solar Analyst [17, 19, 20]. We used estimated average annual atmospheric transmissivity at sea level and diffuse fraction according to the models of Bristow and Campbell (1984) [33] and Carroll (1984) [37] to calculate total monthly solar radiation using Solar Analyst [17, 19, 20]. In addition, hourly solar

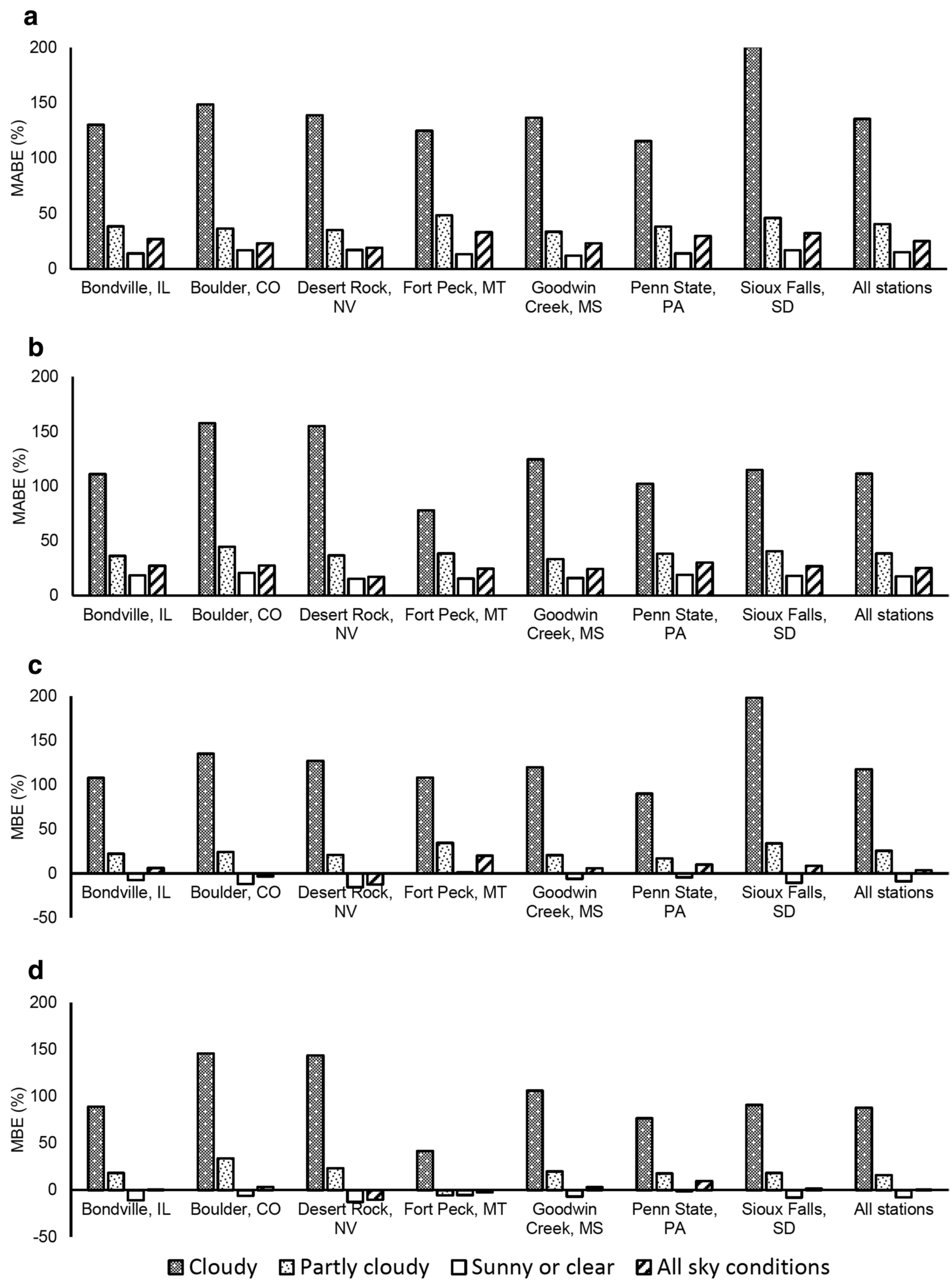

Fig. 3 MABE (%) of the estimated daily atmospheric transmissivity and estimated daily irradiance (**a** and **b**) and also MBE (%) of the estimated daily atmospheric transmissivity and estimated daily irradiance (**c** and **d**) for each sky condition in different sites for the entire study time period

Table 6 Same as Table 5 in 2015

Station name	Daily atmospheric transmissivity					Daily irradiance					n
	MBE		MABE		r	MBE		MABE		r	
	(%)		(%)			(%)	(W m^{-2})	(%)	(W m^{-2})		
All sky conditions											
Bondville, IL	5.49	0.03	39.75	0.20	NSS	− 0.58	− 0.97	27.49	46.50	0.81**	365
Boulder, CO	− 1.93	− 0.01	22.05	0.12	0.50**	5.42	10.02	28.14	52.07	0.80**	365
Desert Rock, NV	− 10.07	− 0.06	17.85	0.11	0.42**	− 5.99	− 13.75	16.10	36.96	0.87**	363
Fort Peck, MT	22.25	0.11	33.66	0.15	0.50**	0.31	0.49	22.64	36.03	0.88**	362
Goodwin Creek, MS	8.36	0.04	22.07	0.10	0.72**	7.25	12.80	23.93	42.28	0.83**	364
Penn State, PA	10.84	0.05	29.86	0.14	0.57**	9.61	15.15	31.00	48.84	0.82**	365
Sioux Falls, SD	7.03	0.04	31.55	0.16	0.18**	2.05	3.39	28.07	46.54	0.81**	365
Combined data from all stations	5.23	0.03	27.51	0.14	0.44**	2.19	3.89	24.89	44.15	0.83**	2549
Daily atmospheric transmissivity ≤ 0.30 (Cloudy sky)											
Bondville, IL	181.88	0.31	197.90	0.34	NSS	79.23	37.31	105.08	49.48	0.70**	72
Boulder, CO	80.19	0.16	93.65	0.18	NSS	87.81	58.79	100.27	67.13	0.42**	39
Desert Rock, NV	120.71	0.26	124.55	0.27	NSS	114.58	69.23	117.61	71.05	0.80**	13
Fort Peck, MT	121.85	0.23	141.60	0.27	0.34**	54.45	25.46	94.30	44.09	0.72**	73
Goodwin Creek, MS	90.68	0.15	108.50	0.18	NSS	82.64	46.45	100.43	56.45	0.55**	85
Penn State, PA	105.79	0.19	121.69	0.22	0.25*	77.68	40.07	98.18	50.65	0.66**	93
Sioux Falls, SD	228.56	0.38	228.56	0.38	NSS	119.93	57.59	141.50	67.95	0.64**	54
Combined data from all stations	130.29	0.24	144.72	0.26	0.14**	82.78	43.16	105.03	54.76	0.63**	431
0.30 < daily atmospheric transmissivity < 0.50 (Partly cloudy sky)											
Bondville, IL	33.93	0.13	51.27	0.20	− 0.24*	23.74	35.40	34.09	50.83	0.84**	84
Boulder, CO	28.00	0.12	42.96	0.18	NSS	39.20	50.90	54.47	70.73	0.84**	71
Desert Rock, NV	20.53	0.08	32.23	0.13	NSS	26.76	38.13	36.88	52.54	0.83**	33
Fort Peck, MT	38.08	0.15	46.14	0.18	NSS	− 4.13	− 4.75	31.57	36.33	0.90**	124
Goodwin Creek, MS	25.85	0.10	36.20	0.14	0.28*	27.26	38.95	38.81	55.46	0.83**	69
Penn State, PA	13.11	0.05	35.72	0.14	0.24*	15.39	20.47	36.50	48.55	0.84**	95
Sioux Falls, SD	29.65	0.11	44.26	0.17	NSS	19.71	25.42	37.31	48.11	0.85**	81
Combined data from all stations	28.18	0.11	42.42	0.17	NSS	18.95	25.06	37.83	50.03	0.85**	555
Daily atmospheric transmissivity ≥ 0.50 (Sunny and clear sky)											
Bondville, IL	− 17.23	− 0.11	22.78	0.15	NSS	− 13.13	− 28.78	19.95	43.73	0.90**	209
Boulder, CO	− 10.75	− 0.07	15.24	0.10	0.21**	− 4.03	− 8.81	20.40	44.57	0.91**	255
Desert Rock, NV	− 13.58	− 0.09	15.63	0.11	0.19**	− 9.19	− 22.56	13.82	33.94	0.92**	317
Fort Peck, MT	5.18	0.03	12.18	0.07	NSS	− 2.73	− 6.61	13.32	32.24	0.88**	165
Goodwin Creek, MS	− 3.9	− 0.02	10.05	0.06	0.28**	− 3.98	− 9.40	13.62	32.22	0.91**	210
Penn State, PA	− 4.36	− 0.02	13.96	0.09	0.16*	− 0.45	− 1.02	21.12	48.02	0.83**	177
Sioux Falls, SD	− 11.14	− 0.07	16.96	0.11	0.19**	− 8.28	− 17.08	19.85	40.97	0.90**	230
Combined data from all stations	− 9.15	− 0.06	15.46	0.10	0.11**	− 6.33	− 14.45	17.18	39.20	0.89**	1563

*Significant in 95% confidence level

**Significant in 99% confidence level

NSS not statistically significant

radiation values can be calculated using the ratio between daily and hourly radiation estimates suggested in the previous literature, combined with the estimated daily insolation from the method presented in this paper. The method was validated using seven different sites in climatologically different areas over the United States. Overall, results showed that daily solar radiation can be estimated very well with MABE of about 40 to 53 W m^{-2} or MBE of ± 10% under all sky conditions between the seven sites using the presented method, which is an improvement over previously used methods with MBE of under 10% because the modified approach and model presented here also require significantly

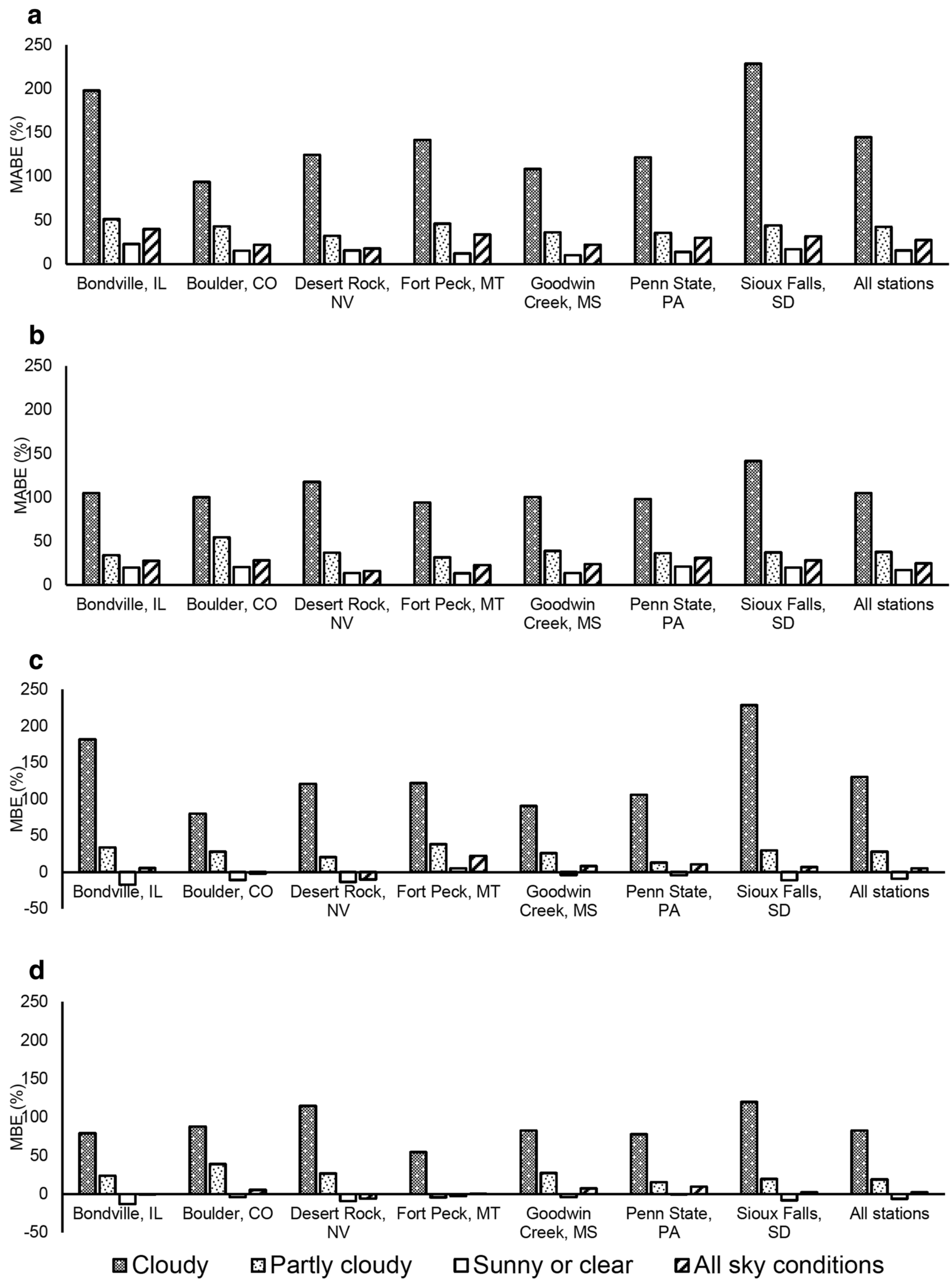

Fig. 4 MABE (%) of the estimated daily atmospheric transmissivity and estimated daily irradiance (**a** and **b**) and also MBE (%) of the estimated daily atmospheric transmissivity and estimated daily irradiance (**c** and **d**) for each sky condition in different sites for 2015

International Journal of Energy and Environmental Engineering (2018) 9:383–398

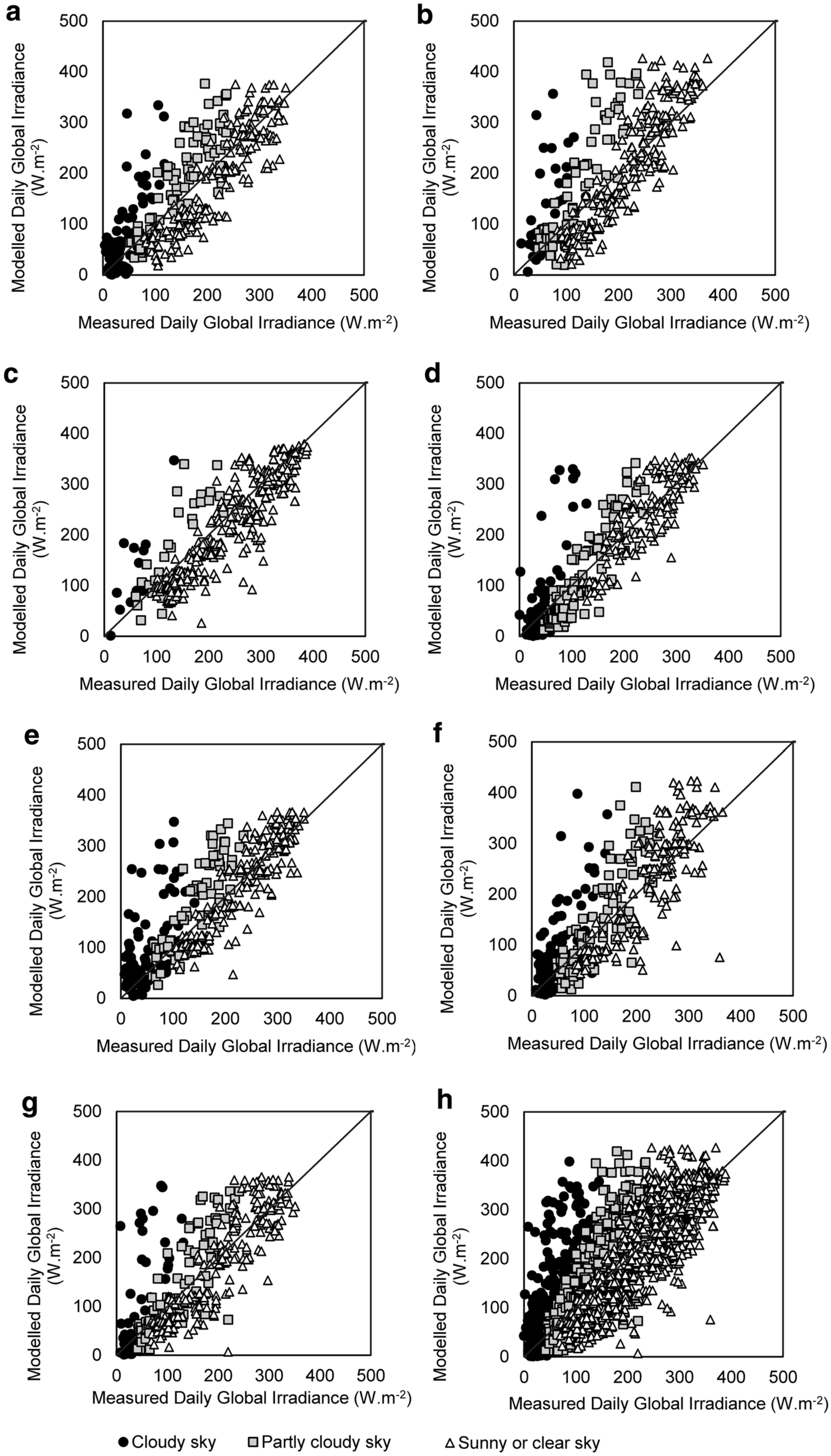

Fig. 5 Comparison of the measured versus predicted daily irradiance (W m^{-2}) for Bondville, IL (**a**), Boulder, CO (**b**), Desert Rock, NV (**c**), Fort Peck, MT (**d**), Goodwin Creek, MS (**e**), Penn State, PA (**f**), Sioux Falls, SD (**g**) and all the SURFRAD stations (**h**) in 2015, as an example of a single year

less input data. This method can be very useful especially for those stations with substantially higher number of sunny days than cloudy or partly cloudy days, assuming the availability of air temperature data. The estimated values for those days that the model is not able to estimate accurately can be corrected using available measured data. The implemented DEM environment of this method makes it applicable in many studies that need spatial estimation of solar radiation, especially solar energy generation projects.

Compliance with ethical standards

Conflict of interest On behalf of all authors, the corresponding author states that there is no conflict of interest.

References

1. Aladenola, O.O., Madramootoo, C.A.: Evaluation of solar radiation estimation methods for reference evapotranspiration estimation in Canada. Theoret. Appl. Climatol. **118**(3), 377–385 (2014). https://doi.org/10.1007/s00704-013-1070-2
2. Kodysh, J.B., Omitaomu, O.A., Bhaduri, B.L., Neish, B.S.: Methodology for estimating solar potential on multiple building rooftops for photovoltaic systems. Sustain Cities Soc **8**, 31–41 (2013). https://doi.org/10.1016/j.scs.2013.01.002
3. McKenney, D.W., Pelland, S., Poissant, Y., Morris, R., Hutchinson, M., Papadopol, P., Lawrence, K., Campbell, K.: Spatial insolation models for photovoltaic energy in Canada. Sol. Energy **82**(11), 1049–1061 (2008). https://doi.org/10.1016/j.solener.2008.04.008
4. Bird, R.E., Hulstrom, R.L.: Simplified clear sky model for direct and diffuse insolation on horizontal surfaces. Solar Energy Res. Inst., Golden (1981)
5. Badescu, V., Gueymard, C.A., Cheval, S., Oprea, C., Baciu, M., Dumitrescu, A., Iacobescu, F., Milos, I., Rada, C.: Computing global and diffuse solar hourly irradiation on clear sky. Review and testing of 54 models. Renew. Sustain. Energy Rev. **16**(3), 1636–1656 (2012)
6. Gueymard, C.A., Ruiz-Arias, J.A.: Validation of direct normal irradiance predictions under arid conditions: a review of radiative models and their turbidity-dependent performance. Renew. Sustain. Energy Rev. **45**, 379–396 (2015)
7. Atwater, M.A., Ball, J.: A numerical solar radiation model based on standard meteorological observations. Sol. Energy **21**(3), 163–170 (1978)
8. Rigollier, C., Bauer, O., Wald, L.: On the clear sky model of the ESRA—European Solar Radiation Atlas—with respect to the Heliosat method. Sol. Energy **68**(1), 33–48 (2000)
9. Ineichen, P.: A broadband simplified version of the Solis clear sky model. Sol. Energy **82**(8), 758–762 (2008)
10. Maxwell, E.L.: METSTAT—the solar radiation model used in the production of the national solar radiation data base (NSRDB). Sol. Energy **62**(4), 263–279 (1998)
11. Gul, M.S., Muneer, T., Kambezidis, H.D.: Models for obtaining solar radiation from other meteorological data. Sol. Energy **64**(1), 99–108 (1998)
12. Muneer, T., Gul, M., Kambezidis, H.: Long-term evaluation of a meteorological solar radiation model against UK data. Energy Convers. Manag. **39**, 303–317 (1998)
13. Nottrott, A., Kleissl, J.: Validation of the NSRDB–SUNY global horizontal irradiance in California. Sol. Energy **84**(10), 1816–1827 (2010)
14. Paulescu, M., Schlett, Z.: A simplified but accurate spectral solar irradiance model. Theoret. Appl. Climatol. **75**(3), 203–212 (2003)
15. Gueymard, C.A.: REST2: high-performance solar radiation model for cloudless-sky irradiance, illuminance, and photosynthetically active radiation–Validation with a benchmark dataset. Sol. Energy **82**(3), 272–285 (2008)
16. Šúri, M., Hofierka, J.: A new GIS-based solar radiation model and its application to photovoltaic assessments. Trans GIS **8**(2), 175–190 (2004)
17. Ruiz-Arias, J., Tovar-Pescador, J., Pozo-Vázquez, D., Alsamamra, H.: A comparative analysis of DEM-based models to estimate the solar radiation in mountainous terrain. Int. J. Geogr. Inf. Syst. **23**(8), 1049–1076 (2009)
18. Miklánek, P., Mészároš, I.: Modelling of insolation characteristics in mountainous environment. Adv. Water Sci. **2**, 32–36 (1993)
19. Dubayah, R., Rich, P.M.: Topographic solar radiation models for GIS. Int. J. Geogr. Inf. Syst. **9**(4), 405–419 (1995). https://doi.org/10.1080/02693799508902046
20. Fu, P., Rich, P.M.: A geometric solar radiation model with applications in agriculture and forestry. Comput. Electron. Agric. **37**(1), 25–35 (2002)
21. Wilson, J.P., Gallant, J.C.: Terrain analysis: principles and applications. Wiley, Hoboken (2000)
22. Zelenka, A., Perez, R., Seals, R., Renné, D.: Effective accuracy of satellite-derived hourly irradiances. Theoret. Appl. Climatol. **62**(3), 199–207 (1999)
23. Kasten, F., Czeplak, G.: Solar and terrestrial radiation dependent on the amount and type of cloud. Sol. Energy **24**(2), 177–189 (1980)
24. Beyer, H.G., Costanzo, C., Heinemann, D.: Modifications of the Heliosat procedure for irradiance estimates from satellite images. Sol. Energy **56**(3), 207–212 (1996)
25. Olatomiwa, L., Mekhilef, S., Shamshirband, S., Mohammadi, K., Petković, D., Sudheer, C.: A support vector machine–firefly algorithm-based model for global solar radiation prediction. Sol. Energy **115**, 632–644 (2015)
26. Sen, Z.: Solar energy fundamentals and modeling techniques: atmosphere, environment, climate change and renewable energy. Springer, Heidelberg (2008)
27. Yacef, R., Mellit, A., Belaid, S., Şen, Z.: New combined models for estimating daily global solar radiation from measured air temperature in semi-arid climates: application in Ghardaïa, Algeria. Energy Convers. Manag. **79**, 606–615 (2014)
28. Gago, E.J., Etxebarria, S., Tham, Y., Aldali, Y., Muneer, T.: Inter-relationship between mean-daily irradiation and temperature, and decomposition models for hourly irradiation and temperature. Int. J. Low-Carbon Technol. **6**(1), 22–37 (2011). https://doi.org/10.1093/ijlct/ctq039
29. Quan, D.M., Ogliari, E., Grimaccia, F., Leva, S., Mussetta, M.: Hybrid model for hourly forecast of photovoltaic and wind power. In: Fuzzy Systems (FUZZ), 2013 IEEE International Conference on 2013, pp. 1–6. IEEE

30. Ogliari, E., Grimaccia, F., Leva, S., Mussetta, M.: Hybrid predictive models for accurate forecasting in PV systems. Energies **6**(4), 1918–1929 (2013)
31. Collares-Pereira, M., Rabl, A.: The average distribution of solar radiation-correlations between diffuse and hemispherical and between daily and hourly insolation values. Sol. Energy **22**(2), 155–164 (1979)
32. Myers, D.R.: Solar radiation modeling and measurements for renewable energy applications: data and model quality. Energy **30**(9), 1517–1531 (2005)
33. Bristow, K.L., Campbell, G.S.: On the relationship between incoming solar radiation and daily maximum and minimum temperature. Agric. For. Meteorol. **31**(2), 159–166 (1984)
34. Liu, B.Y., Jordan, R.C.: The interrelationship and characteristic distribution of direct, diffuse and total solar radiation. Sol. Energy **4**(3), 1–19 (1960)
35. Tham, Y., Muneer, T., Davison, B.: Estimation of hourly averaged solar irradiation: evaluation of models. Build. Serv. Eng. Res. Technol. **31**(1), 9–25 (2010)
36. Page, J.K.: Prediction of solar radiation on inclined surfaces, vol. 3. Springer, Heidelberg (1986)
37. Carroll, J.: Global transmissivity and diffuse fraction of solar radiation for clear and cloudy skies as measured and as predicted by bulk transmissivity models. Sol. Energy **35**(2), 105–118 (1985)
38. Thornton, P.E., Running, S.W.: An improved algorithm for estimating incident daily solar radiation from measurements of temperature, humidity, and precipitation. Agric. For. Meteorol. **93**(4), 211–228 (1999)
39. Hungerford, R.D., Nemani, R.R., Running, S.W., Coughlan, J.C.: MTCLIM: a mountain microclimate simulation model. Res. Pap. INT-RP-414, p. 52. US Department of Agriculture, Forest Service, Intermountain Research Station, Ogden, UT (1989)
40. Colli, A., Pavanello, D., Zaaiman, W.J., Heiser, J., Smith, S.: Statistical analysis of weather conditions based on the Clearness Index and correlation with meteorological variables. Int. J. Sustain. Energy 35(6), 523–536 (2016)
41. Spencer, J.: Fourier series representation of the position of the sun. Search **2**(5), 172–173 (1971)
42. Whillier, A.: The determination of hourly values of total solar radiation from daily summations. Theoret. Appl. Climatol. **7**(2), 197–204 (1956)
43. Hawas, M., Muneer, T.: Study of diffuse and global radiation characteristics in India. Energy Convers. Manag. **24**(2), 143–149 (1984)
44. Augustine, J.A., DeLuisi, J.J., Long, C.N.: SURFRAD—A national surface radiation budget network for atmospheric research. Bull. Am. Meteor. Soc. **81**(10), 2341–2357 (2000)
45. Augustine, J.A., Hodges, G.B., Cornwall, C.R., Michalsky, J.J., Medina, C.I.: An update on SURFRAD—The GCOS surface radiation budget network for the continental United States. J. Atmos. Ocean. Technol. **22**(10), 1460–1472 (2005)
46. NASA LP DAAC: Advanced spaceborne thermal emission and reflection radiometer (ASTER) global digital elevation model. In: NASA EOSDIS land processes DAAC, U.E.R.O.a.S.E.C.h.l.u.g. (ed.). (2011)
47. Willmott, C.J., Matsuura, K.: Advantages of the mean absolute error (MAE) over the root mean square error (RMSE) in assessing average model performance. Climate Res **30**(1), 79–82 (2005)